

# Longitudinal muon spin relaxation in high purity aluminum and silver

J.F. Bueno,<sup>1</sup> D.J. Arseneau,<sup>2</sup> R. Bayes,<sup>2,\*</sup> J.H. Brewer,<sup>1</sup> W. Faszer,<sup>2</sup> M.D. Hasinoff,<sup>1</sup> G.M. Marshall,<sup>2</sup>  
E.L. Mathie,<sup>3</sup> R.E. Mischke,<sup>2,†</sup> G.D. Morris,<sup>2</sup> K. Olchanski,<sup>2</sup> V. Selivanov,<sup>4</sup> and R. Tacik<sup>3</sup>

<sup>1</sup>*University of British Columbia, Vancouver, British Columbia, V6T 1Z1, Canada*

<sup>2</sup>*TRIUMF, Vancouver, British Columbia, V6T 2A3, Canada*

<sup>3</sup>*University of Regina, Regina, Saskatchewan, S4S 0A2, Canada*

<sup>4</sup>*Kurchatov Institute, Moscow, 123182, Russia*

(Dated: January 13, 2013)

The time dependence of muon spin relaxation has been measured in high purity aluminum and silver samples in a longitudinal 2 T magnetic field at room temperature, using time-differential  $\mu^+$ SR. For times greater than 10 ns, the shape fits well to a single exponential with relaxation rates of  $\lambda_{Al} = 1.3 \pm 0.2$  (stat.)  $\pm 0.3$  (syst.)  $\text{ms}^{-1}$  and  $\lambda_{Ag} = 1.0 \pm 0.2$  (stat.)  $\pm 0.2$  (syst.)  $\text{ms}^{-1}$ .

PACS numbers: 76.75.+i

## I. INTRODUCTION

When positive muons are stopped in a high purity metal with the muon spin along the direction of an applied magnetic field, the muons can be depolarized by interactions with nuclear dipole moments, conduction electrons, and paramagnetic impurities. The form of the resulting depolarization has been studied using the  $\mu^+$ SR technique,<sup>1</sup> but has not been quantified to the level needed for the TWIST experiment,<sup>2</sup> in which the absolute polarization of the muons must be known with high precision. TWIST used stopping targets of aluminum and silver with purity greater than 99.999% immersed in an external 2.0 T longitudinal magnetic field at room temperature. Because the TWIST drift chamber detector system recorded ionization from incoming muons as well as positrons with a relatively slow drift gas, the analysis discarded decay positrons within 1.05  $\mu\text{s}$  of the muon stopping time due to possible time overlap of muon and positron ionization. Therefore, a time differential  $\mu^+$ SR experiment was undertaken to make a precise measurement of the relaxation rate, especially for decay times below 1.05  $\mu\text{s}$ .

## II. DEPOLARIZATION MECHANISMS FOR STOPPED MUONS

After motional thermalization, positive muons are limited to interstitial and substitutional sites. When nearly thermalized, a muon in a good metal attracts a screening charge of conduction electrons.<sup>3</sup> At room temperature, a muon is usually diffusing between energetically allowed sites before decaying. The conduction electrons in aluminum and silver efficiently screen the ionic potentials over all distances greater than the Fermi-Thomas screening length.

Muons can become trapped at crystal defects, of which there are a wide variety; the most common originate from the manufacturing process, such as when a metal is cold-rolled to produce a thin foil. Trapping by such

defects makes the muon mobility strongly sample dependent. The defects are enhanced by quenching, and can be diminished by annealing.

In slowing down from high energy, the muon itself can cause lattice defects as it imparts recoil energy to lattice ions in  $\sim 10^{-17}$  s and the lattice distributes this energy to neighbouring atoms in  $\sim 10^{-12}$  s.<sup>4</sup> A nucleus can be knocked out of its lattice position into an interstitial site, leaving a vacancy (Frenkel defect). However, these vacancies are unlikely to affect the muon's diffusion, since the muon thermalizes  $\sim 1$   $\mu\text{m}$  from the last defect introduced.<sup>5</sup>

The magnetic field experienced by a stationary muon due to the magnetic dipole moments of nuclei and lattice impurities can be modelled as static, isotropic, and Gaussian. If the muon samples a new field taken at random from the same distribution every time it “hops” to a new lattice site, the resulting depolarization is given by<sup>6</sup>

$$P_\mu(t) = P_\mu(0) \exp \left\{ -\frac{2\Delta^2}{\nu^2} [\exp(-\nu t) - 1 + \nu t] \right\}, \quad (1)$$

and is valid for  $\nu/\Delta$  sufficiently large, where  $\Delta$  is a measure of the magnetic field distribution and  $1/\nu$  is the mean time between muon hops. Each field component is presumed to have an independent Gaussian distribution  $\mathcal{D}(B_{\text{local}}) \sim \exp[-B_{\text{local}}^2/(2\Delta^2/\gamma_\mu^2)]$ , where  $\gamma_\mu$  is the muon's gyromagnetic ratio and  $\Delta/\gamma_\mu$  is the standard deviation of a Gaussian distribution of magnetic fields.

If an external field  $\vec{B}_{\text{ext}}$  is now applied in a direction *transverse* to the muon polarization, the muon spins precess and are depolarized according to the Abragam formula:<sup>7</sup>

$$P_\mu(t) = P_\mu(0) \exp \left\{ -\frac{\Delta^2}{\nu^2} [\exp(-\nu t) - 1 + \nu t] \right\} \cos(\omega_\mu t), \quad (2)$$

where  $\omega_\mu = \gamma_\mu B_{\text{ext}}$ . In the “motional narrowing” limit, the muons move quickly so that  $\nu$  is large,  $\exp(-\nu t) \rightarrow 0$  and the *envelope* of Eq. (2) approaches an exponential time dependence. In the static limit, the envelope instead approaches a Gaussian time dependence.

If a *longitudinal* field  $B_0$  is applied, the static relaxation function becomes<sup>8</sup>

$$P_\mu(t) = 1 - \frac{2\Delta^2}{\omega_0^2} \left[ 1 - \exp\left(-\frac{1}{2}\Delta^2 t^2\right) \cos \omega_0 t \right] + \frac{2\Delta^4}{\omega_0^3} \int_0^t \exp\left(-\frac{1}{2}\Delta^2 \tau^2\right) \sin \omega_0 \tau d\tau, \quad (3)$$

where  $\omega_0 = \gamma_\mu B_0 \approx 272$  MHz, and the longitudinal field is seen to suppress the depolarization due to nuclear dipole moments. The largest observed nuclear dipolar field on a muon in a crystal is  $\Delta/\gamma_\mu = 0.47$  mT,<sup>9</sup> while the applied longitudinal field in this experiment was  $B_0 = 2$  T, so that  $(2\Delta^2/\omega_0^2) \lesssim 10^{-7}$ . Of course, in our experiment the muons are not static. The cumulative loss of polarization increases with increasing  $\nu$  as long as  $\nu \ll \omega_0$ . For  $\nu \gg \omega_0$  “motional averaging” sets in and the relaxation rate goes down again; this is known as the “ $T_1$  minimum” effect.<sup>10</sup> So the fastest relaxation would be for  $\nu \sim 100 \mu\text{s}^{-1}$ ; assuming muons lose up to  $10^{-7}$  of their polarization at each hop, in that case the relaxation rate is  $< 0.01 \text{ ms}^{-1}$ . At room temperature in aluminum<sup>11</sup>  $\nu \approx 10^{11} \text{ s}^{-1}$ , which is far past the “ $T_1$  minimum”. Depolarization by nuclear dipole moments is therefore negligible for this experiment.

Korringa relaxation<sup>12</sup> caused by a hyperfine contact interaction between the muon spin and fluctuating conduction electron spins is the most likely cause of any muon depolarization in this experiment. The net hyperfine coupling is an average over all electron spin orientations.<sup>13,14</sup> The resulting exponential relaxation rate is given by

$$P_\mu(t) = P_\mu(0) \exp(-\lambda t). \quad (4)$$

where  $\lambda$  is proportional to  $K_\mu^2 T$ . The muon Knight shift  $K_\mu = (\omega - \omega_0)/\omega_0$  is the fractional muon frequency shift due to the same hyperfine interaction. Korringa relaxation has been observed in several non-magnetic metals (lead, cadmium, zinc, copper), where the muon relaxation rates increase linearly with temperature and are robust to field changes in the range 0.01 T to 0.20 T,<sup>15</sup> as expected.<sup>13</sup>

As we have seen, relaxation of muons by nuclear dipole moments is heavily suppressed by a longitudinal magnetic field. The electronic dipole moments of paramagnetic ions are much larger and can produce fields up to 0.1 T at a distance of one lattice spacing.<sup>16,17</sup> Thus they are much more difficult to decouple from the muon and may cause exponential relaxation of muons in a crystal with significant concentrations of paramagnetic impurities.<sup>7,16,18</sup>

In summary, muon spin relaxation due to nuclear dipole moments exhibits an exponential form when the muons hop rapidly, as expected at room temperature. Non-exponential static dipolar relaxation may occur if the muons become trapped at defects or vacancies, which is possible in our aluminum foil since it was not annealed, but any such static relaxation due to nuclear dipole moments is heavily suppressed by the presence of a strong

longitudinal magnetic field. In the silver foil, trapping at paramagnetic impurities cannot be excluded. The appropriate form is still exponential, as long as the muons diffuse sufficiently fast to find the impurities promptly. This may be the case in an annealed sample such as our silver foil. For both foils, Korringa relaxation is expected to be the dominant mechanism for depolarization.

### III. PREVIOUS MEASUREMENTS

We were unable to find any measurements from  $\mu^+$ SR taken under conditions comparable to those of TWIST. Depolarization in aluminum and silver from nuclear dipole moments has been measured in  $\mu^+$ SR experiments, using a transverse magnetic field arrangement. There are more studies on aluminum since its nuclear dipole moment is about 35 times larger than silver. Even with its large dipole moment, high purity aluminum leads to almost negligible depolarization down to 1 K.<sup>19–23</sup> Consequently, a measurable depolarization is typically seen only in samples that have been doped with impurities.<sup>3,24,25</sup>

There is a contradictory measurement,<sup>26</sup> which used aluminum and silver targets of 99.99% purity in a transverse field arrangement, at room temperature, and observed a Gaussian form for the depolarization in aluminum. They explained this anomalous result as due to muons trapping in defects, which originated from the cold-rolling during manufacture of the foil.<sup>27</sup>

The result from an intermediate phase of TWIST,<sup>17</sup> which used a 2 T longitudinal magnetic field, is  $\lambda_{\text{Al}} = 1.6 \pm 0.3 \text{ ms}^{-1}$ . One other measurement<sup>28</sup> was available prior to this experiment, where a high purity aluminum sample was measured in a 1.1 T longitudinal field. The result, based on four points in the time range of 0.1 to 10  $\mu\text{s}$ , is  $\lambda_{\text{Al}} = 0.43 \pm 0.34 \text{ ms}^{-1}$ . It is difficult to compare the results from these two experiments due to differences in magnetic fields, limited statistical precision, and suspected systematic uncertainties in determining  $\lambda$ . Comparing results between different experiments has the additional complication that if the depolarization is dominated by small impurities and/or defects introduced during manufacturing, then the result is expected to be dependent on the sheet from which the sample is taken.

### IV. EXPERIMENTAL DETAILS

In December 2006 we acquired  $\mu^+$ SR data using the facilities of the TRIUMF Centre for Molecular & Materials Science. The M20B beamline, which was a dedicated surface muon channel,<sup>29</sup> included collimators for the muons and a DC separator that removed positrons by velocity selection. The separator also rotated the muon spin by  $11^\circ$ , creating a small transverse polarization component and reducing the longitudinal polarization by 2%. The muon rate was typically 20–40 kHz. The muon target

and positron counters are shown schematically in Fig. 1. Muons could stop in the sample under investigation, one of the scintillators, or an Ag mask of purity 99.99%. Most data were taken with a TM2 scintillator of nominal thickness 254  $\mu\text{m}$ , but data were also taken with nominal thicknesses of 127 and 508  $\mu\text{m}$ . The backward (B) and forward (F) positron counters were approximately 0.6 cm thick. The backward counter was a disc of about 8.0 cm diameter, with a 2.5 cm hole for the muon beam. The F counter was tubular, with inner diameter of 10.5 cm and length 35.5 cm. The target module was placed in the HELIOS superconducting solenoid that supplied a longitudinal 2 T magnetic field over the stopping target. The target was at room temperature, and the region around the target was evacuated.

The aluminum stopping target was purchased from Goodfellow Corporation,<sup>30</sup> who specified the typical impurities as 0.3 ppm of Cu, 0.3 ppm of Fe, 1.2 ppm of Mg, and 0.8 ppm of Si. In aluminum, the muons are not trapped by impurities above  $\approx 100$  K.<sup>23</sup> High purity aluminum has been studied under annealing and quenching,<sup>31</sup> over a temperature range of 19 to 900 K: most defects were found to be absent after allowing the quenched sample to reach room temperature. The silver stopping target was purchased from ESPI Metals,<sup>32</sup> who specified the typical impurities as 2 ppm of Fe, < 2 ppm of Bi, 0.6 ppm of Cu, and 0.6 ppm of Pd. It was annealed in an inert argon atmosphere, after machining. In silver, there is evidence that room temperature trapping at impurities can occur,<sup>18</sup> but that would not be of consequence for our annealed sample.

The data acquisition system recorded the positron time of arrival relative to that of the muon, in two pairs of histograms, each with 19200 channels of width 0.78125 ns. Data were recorded for the B and F counters, in parallel for muons stopping in the Ag mask and for those stopping in the target, separated by the absence or presence of a signal in TM2 (see Fig. 1). There was a background of muon decays in or near the collimator, scattered positrons, and muon decays between the muon detector and the target. The electronics removed the background from muon pile-up, where a second muon enters the sample region during the same 15  $\mu\text{s}$  long data gate as the original muon. The positron gate was open for 1  $\mu\text{s}$  before the muon trigger, so that events were recorded that could not possibly be caused by decay of the detected muon. The aim was to fix the background to the average of the number of decays recorded in this 1  $\mu\text{s}$  interval.

The stopping targets are listed in Table I. For sets E-K, the target consisted of two layers, one of metal from the same foils as the TWIST targets, the other a calibration sample (CS). The orientation of the layers could be reversed to expose either one to the stopping muon beam. The metal portion was either 10 folded layers of Al or 6 folded layers of Ag, both of which were sufficiently thick to stop all the muons in the surface muon beam. The layers were bound together with 3.6  $\mu\text{m}$  thickness

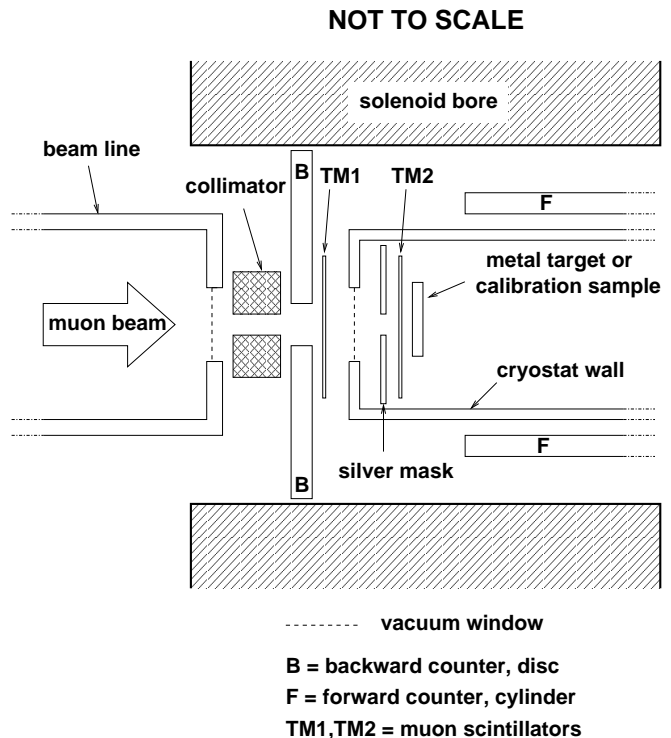


FIG. 1. Schematic for the experiment. A collimated muon beam enters from the left and muon decays are recorded in one set of histograms if they are detected only by the first scintillator (TM1), stopping mostly in the Ag mask, or in another set of histograms if they are recorded by both scintillators (TM1 and TM2), mostly stopping in the target. The backward positron counter (B) is protected from the muon beam by a collimator. Materials such as the photomultiplier tubes and light guides are not shown.

Mylar. The CS was a 2.5 cm diameter, 0.2 cm thick (mass 4.6g) pressed powder disc of  $\text{Gd}_2\text{Ti}_2\text{O}_7$ , a geometrically frustrated antiferromagnetic pyrochlore. At room temperature  $\text{Gd}_2\text{Ti}_2\text{O}_7$  is a paramagnet in which fluctuating magnetic moments are known to depolarize muon spins within a few microseconds, with an exponential form of  $P_\mu(t)$ .<sup>33</sup> Note that no grease or glue was used in the assembly of the targets. Sets A-D used targets of pure CS or pure metal, before we realized the importance of maintaining constant material thickness in the decay positron path when making systematic comparisons of decay asymmetry. We anticipated that determining the fraction of muons stopping in the trigger scintillator (TM2) would be a dominant source of systematic uncertainty, thus for sets I-K the thickness of the trigger scintillator was altered.

## V. ANALYSIS

When analyzed with a Fourier transform algorithm, the data showed time structures with periods of 43.37 ns

TABLE I. Data sets for the  $\mu^+$ SR experiment. Sets C and D had a low muon rate. Set D had the DC separator on a high setting. In the target column, the upstream material of the reversible target is listed first.

Data set	Target	Scintillator thickness ( $\mu\text{m}$ )	Duration (hours)	$\mu^+$ counts Ag mask ( $\times 10^9$ )	$\mu^+$ counts sample ( $\times 10^9$ )
A	CS <sup>a</sup>	254	14.1	1.2	0.8
B	Al	254	8.0	0.7	0.5
C	Al	254	15.7	0.7	0.5
D	Al	254	5.7	0.3	0.2
E	CS+Al	254	24.0	1.7	1.2
F	Al+CS	254	40.1	2.9	2.0
G	Ag+CS	254	32.4	2.5	1.7
H	CS+Ag	254	22.8	1.8	1.2
I	CS+Ag	508	18.0	1.3	0.9
J	CS+Ag	127	22.2	1.5	1.0
K	Ag+CS	127	13.3	1.0	0.7

<sup>a</sup> CS:  $\text{Gd}_2\text{Ti}_2\text{O}_7$  calibration sample

and 3.68 ns, corresponding to the period of the TRIUMF cyclotron and the precession frequency of the muon transverse polarization components in the 2.0 T magnetic field. To minimize the impact of possible effects, we rebinned our data using time bins of width 89.84 ns starting 10 ns after the muon stop time, and we later verified that our results are robust to the binning used.

We simultaneously fit the B and F decay count histograms with standard coupled  $\mu^+$ SR equations,

$$n_b(t) = b_b + N_0 e^{-t/\tau_\mu} [1 + A_b P_\mu(t)] \quad (5)$$

$$n_f(t) = b_f + r N_0 e^{-t/\tau_\mu} [1 + A_f P_\mu(t)], \quad (6)$$

where  $n_b$  and  $n_f$  are the number of B and F counts,  $b_b$  and  $b_f$  are the backgrounds in each counter,  $\tau_\mu = 2.19703 \mu\text{s}$  is the muon lifetime,  $N_0$  is the histogram normalization,  $A_b$  and  $A_f$  are the empirical asymmetries that depend only on the counter geometry and the material through which the decay positrons pass. The parameter  $r$  is introduced to account for differences between the B and F counters' energy and angular acceptance. The CS sample was fit first, using three forms for the depolarization: a single exponential,  $P_\mu(t) = P_\mu(0) \exp(-\lambda t)$ , a sum of two exponentials, and a power law,  $P_\mu(t) = \exp(-at^p)$ . The data were consistent with a single exponential relaxation, so this form is assumed in the following. (See Fig. 2.)

The backgrounds in each counter were determined using the  $1 \mu\text{s}$  of pre-trigger data, and also by leaving the background as a free fit parameter. We found that the two measurements differed by more than three standard deviations, probably due to contamination of the background from long-lived muons. Since the backgrounds could be well determined using the decay data and had a weak correlation with the other fit parameters, we chose to fit the background level with a free parameter.

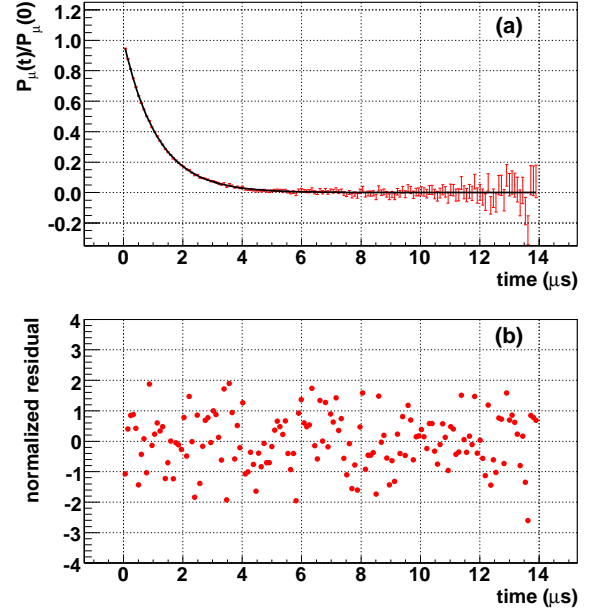


FIG. 2. Depolarization for the CS ( $\text{Gd}_2\text{Ti}_2\text{O}_7$ ). (a) relative polarization and (b) normalized residuals. The fit is  $P_\mu(t)/P_\mu(0) = \exp(-\lambda t)$  to data from set E, with  $\lambda = (0.860 \pm 0.004) \mu\text{s}^{-1}$  and the  $\chi^2/\text{ndf} = 285.5/302$ .

## VI. RESULTS AND SYSTEMATIC UNCERTAINTIES

The parameters from fits to data for the Ag mask, which only required a trigger in TM1, were affected by changes in the target and running conditions. This dependence was seen dominantly in the values of the parameter  $r$ . The value of  $\lambda$  was somewhat sensitive to the target, but the average measured value of  $\lambda_{\text{mask}} = (1.07 \pm 0.07) \text{ms}^{-1}$  agrees with the result for the high purity Ag given below. Systematic errors were not evaluated for the Ag mask.

We used the data from sets I and J to determine the relaxation rate for muons stopping in the trigger scintillator. Initially the data with a  $127 \mu\text{m}$  thickness scintillator were fit assuming that all muons passed through the scintillator and stopped in the CS. With the CS relaxation fixed, we fit a sum of exponentials to the data with scintillator thickness  $508 \mu\text{m}$ , which provided an estimate of the relaxation within the scintillator itself. This process was iterated, and we found that a single exponential is adequate to describe the scintillator depolarization, with  $86.0 \pm 0.3\%$  of the muons stopping in the  $508 \mu\text{m}$  thickness scintillator and  $\lambda_{\text{scint}} = (0.0132 \pm 0.0008) \mu\text{s}^{-1}$ . Then the CS relaxation is  $\lambda_{\text{CS}} = (0.866 \pm 0.008) \mu\text{s}^{-1}$ . With the relaxation rate for the scintillator component fixed, an attempt was made to determine the fraction of muons stopping in the other two scintillators. For the  $127 \mu\text{m}$  thickness scintillator we find  $(4 \pm 9)\%$ , and for the  $254 \mu\text{m}$  scintillator we find  $(0 \pm 10)\%$  for set E and  $(8 \pm 8)\%$  for

set H. These results are clearly imprecise, so we resorted to an evaluation of the fraction using a SRIM<sup>34</sup> simulation of the muon stopping position distribution. Based on estimates of the M20B beam line mean momentum (between 29.2 and 28.7 MeV/c) and momentum resolution (between 1 and 2%), and of materials in the path of the stopping muons, the results of the simulation showed that  $(3 \pm 3)\%$  of the muons could have stopped in the  $254\text{ }\mu\text{m}$  scintillator, and no more than 0.2% in the  $127\text{ }\mu\text{m}$  scintillator. We correct our result assuming that 3% of muons stop and depolarize in the  $254\text{ }\mu\text{m}$  TM2 trigger scintillator rather than the metal target, and assign a large systematic uncertainty that allows for between 1% and 6% of muons stopping in the scintillator.

The empirical coefficients ( $A_b$  and  $A_f$ ) from the CS analysis were determined with statistical precision  $< 0.3\%$  and were constrained to be  $A_b = 0.185$  and  $A_f = -0.238$  while fitting the asymmetry data for the metals. There is a negligible contribution to the systematic uncertainty from the fixed  $A_b$  and  $A_f$  values; a change of 10% in either of these parameters altered the relaxation rate by at most  $0.12\text{ ms}^{-1}$ . The  $r$  parameter was left free since it was found to be highly sensitive to the exact placement of the target. This is shown in Fig. 3, which also includes the results for the relaxation parameter  $\lambda$  in Eq. (4).

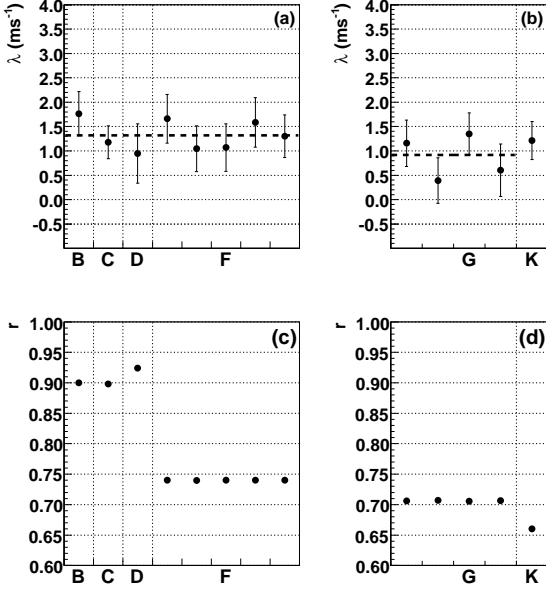


FIG. 3. Results for fits to the metal samples. (a)  $\lambda$  for Al, (b)  $\lambda$  for Ag, (c)  $r$  for Al, and (d)  $r$  for Ag. Sets F and G had multiple runs. The parameter  $r$  is highly sensitive to target placement, which occurred at the beginning of each set.

A significant time structure of the background would give rise to a systematic uncertainty. Because the confidence levels for the fits were reasonable, except for one set that still produced a consistent relaxation rate, there was no need to investigate a possible time structure of

the background. Also, the sets with different muon rates and DC separator settings showed no evidence of an inconsistent relaxation rate. Therefore no systematic uncertainties are assigned for these effects.

The uncertainty in the fraction of muons stopping in the  $254\text{ }\mu\text{m}$  scintillator is much larger than anticipated, and dominates all others. Unfortunately we cannot reduce this uncertainty, since a precise measurement of the M20B mean momentum and resolution was not taken with our beamline settings.

Our results for the  $254\text{ }\mu\text{m}$  scintillator are then

$$\lambda_{\text{Al}} = 1.3 \pm 0.2 \text{ (stat.)} \pm 0.3 \text{ (syst.) ms}^{-1} \text{ and} \quad (7)$$

$$\lambda_{\text{Ag}} = 0.9 \pm 0.2 \text{ (stat.)} \pm 0.2 \text{ (syst.) ms}^{-1}. \quad (8)$$

A single exponential fit is shown for an aluminum run in Fig. 4 and for a silver run in Fig. 5. There is no evidence that anything beyond a single exponential is needed to describe the depolarization. There is no observable fast depolarization component below  $1\text{ }\mu\text{s}$ .

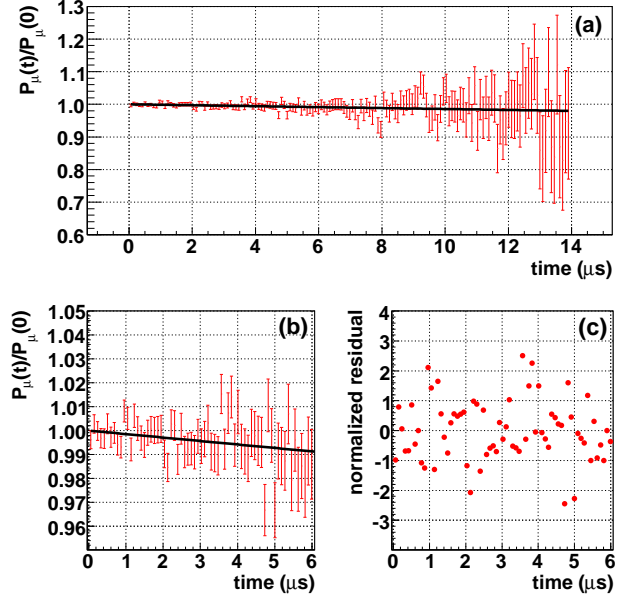


FIG. 4. Aluminum relative polarization vs time. (a) full time range, (b) first 6  $\mu\text{s}$ , and (c) normalized residuals from fit. The fit is  $P_\mu(t)/P_\mu(0) = \exp(-\lambda t)$  to one run of set F, with  $\lambda = (1.5 \pm 0.5)\text{ ms}^{-1}$  and the  $\chi^2/\text{ndf} = 280.6/304$ .

For the single run with the thin ( $127\text{ }\mu\text{m}$ ) scintillator, the contribution from scintillator stops is negligible, but the statistical uncertainty dominates so that

$$\lambda_{\text{Ag}} = 1.2 \pm 0.4 \text{ (stat.) ms}^{-1}. \quad (9)$$

Combining the two results for silver yields

$$\lambda_{\text{Ag}} = 1.0 \pm 0.2 \text{ (stat.)} \pm 0.2 \text{ (syst.) ms}^{-1}. \quad (10)$$

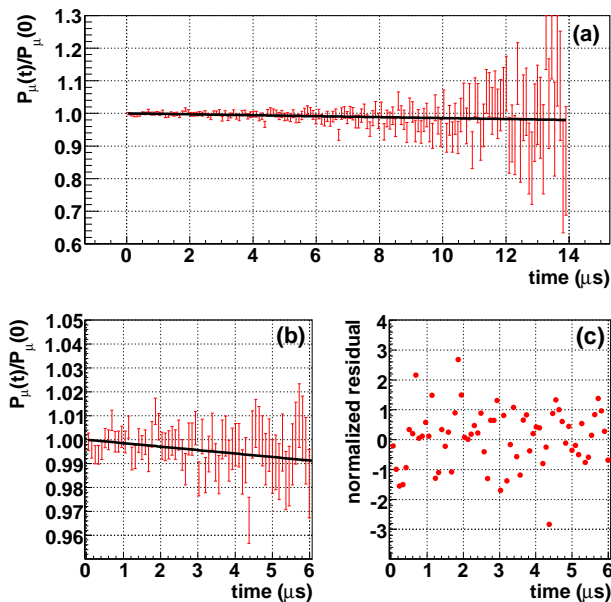


FIG. 5. Silver relative polarization vs time. (a) full time range, (b) first 6  $\mu\text{s}$ , and (c) normalized residuals from fit. The fit is  $P_\mu(t)/P_\mu(0) = \exp(-\lambda t)$  to one run of set G, with  $\lambda = (1.5 \pm 0.5) \text{ ms}^{-1}$  and the  $\chi^2/\text{ndf} = 300.2/304$ .

## VII. CONCLUSIONS

The measured relaxation rates for silver and aluminum differ by less than a factor of two, yet the nuclear dipole moments differ by a factor of 35, providing further evidence that the depolarization is not from nuclear dipole moments. These results are consistent with those from the final phase of the TWIST experiment,<sup>35</sup> but with somewhat larger uncertainties. The unique conclusion from this experiment is that no additional depolarization components exist in the time range  $0.010 < t < 1.000 \mu\text{s}$ ; this is very important for the interpretation of TWIST data. We are unaware of any experimental technique that would allow us to readily study the depolarization below 10 ns, but we are also unaware of any credible models for muon depolarization within the first 10 ns in nonmagnetic metals.

## ACKNOWLEDGMENTS

We thank the staff of the TRIUMF Center for Molecular and Materials Science and our TWIST collaborators for their encouragement and support. In particular, the assistance of B. Hitti, R. Abasalti, and D. Vyas is gratefully acknowledged. This work was supported in part by the Natural Sciences and Engineering Research Council and the National Research Council of Canada, the Russian Ministry of Science, and the U.S. Department of Energy.

- 
- \* Present Address: School of Physics and Astronomy, University of Glasgow, Glasgow, G12 8QQ, Scotland  
 † mischke@triumf.ca
- <sup>1</sup> J. H. Brewer, Muon spin rotation/relaxation/resonance, in *Encyclopedia of Applied Physics* (VCH, New York, 1994), Vol. 11, p. 23.
  - <sup>2</sup> R. Bayes *et al.*, Phys. Rev. Lett. **106**, 041804 (2011).
  - <sup>3</sup> S.F.J. Cox, J. Phys. C: Solid State Phys. **20**, 3187 (1987).
  - <sup>4</sup> W. Schilling, Hyperfine Interactions **4**, 636 (1978).
  - <sup>5</sup> D.K. Brice, Phys. Lett. **66A**, 53 (1978).
  - <sup>6</sup> P. Dalmas de Réotier and A. Yaouanc, J.Phys.: Condens. Matter **9**, 9113 (1997).
  - <sup>7</sup> A. Abragam, Principles of Nuclear Magnetism, in *International series of monographs on physics* (Oxford University Press, 1961).
  - <sup>8</sup> R.S. Hayano, Y.J. Uemura, J. Imazato, N. Nishida, T. Yamazaki, and R. Kubo, Phys. Rev. B **20**, 850 (1979).
  - <sup>9</sup> P. Dalmas de Réotier and A. Yaouanc, J.Phys.: Condens. Matter **4**, 4533 (1992).
  - <sup>10</sup> C.P. Slichter, *Principles of Magnetic Resonance* (Springer-Verlag, Berlin, 1978).
  - <sup>11</sup> D. Richter, Hyperfine Interactions **31**, 169 (1986).
  - <sup>12</sup> J. Korrynga, Physica **16**, 601 (1950).
  - <sup>13</sup> S.J. Blundell and S.F.J. Cox, J. Phys.: Condens. Matter **13**, 2163 (2001).

- <sup>14</sup> J.H. Brewer *et al.*, Positive Muons and Muonium in Matter, in *Muon Physics*, eds. Vernon W. Hughes and C.S. Wu (Academic Press, New York, 1975).
- <sup>15</sup> S.F.J. Cox, S.P. Cottrell, M. Charlton, P.A. Donnelly, S.J. Blundell, J.L. Smith, J.C. Cooley, and W.L. Hulst, Physica B **289-290**, 594 (2000).
- <sup>16</sup> J.A. Brown *et al.*, Phys. Rev. Lett. **47**, 261 (1981).
- <sup>17</sup> B. Jamieson *et al.*, Phys. Rev. D **74**, 072007 (2006).
- <sup>18</sup> R.H. Heffner, Hyperfine Interactions **8**, 655 (1981).
- <sup>19</sup> W.J. Kossler *et al.*, Phys. Rev. Lett. **41**, 1558 (1978).
- <sup>20</sup> O. Hartmann, E. Karlsson, L.O. Norlin, D. Richter, and T.O. Niinikoski, Phys. Rev. Lett. **41**, 1055 (1978).
- <sup>21</sup> K.W. Kehr *et al.*, Phys. Rev. B **26**, 567 (1982).
- <sup>22</sup> K.W. Kehr, Hyperfine Interactions **17-19**, 63 (1984).
- <sup>23</sup> O. Hartmann *et al.*, Phys. Rev. B **37**, 4425 (1988).
- <sup>24</sup> O. Hartmann, Hyperfine Interactions **64**, 641 (1990).
- <sup>25</sup> O. Hartmann *et al.*, Phys. Rev. Lett. **44**, 337 (1980).
- <sup>26</sup> D.P. Stoker *et al.*, Phys. Rev. Lett. **54**, 1887 (1985).
- <sup>27</sup> D.P. Stoker, University of California, Irvine, USA. Private communication, 2009.
- <sup>28</sup> A. Jodidio *et al.*, Phys. Rev. D **34**, 1967 (1986); **37**, 237(E) (1988).
- <sup>29</sup> J. L. Beveridge *et al.*, Nucl. Instrum. Methods A **240**, 316 (1985).
- <sup>30</sup> Goodfellow Corporation, 305 High Tech Drive, Oakdale, PA 15071-3911, USA.

- <sup>31</sup> W.B. Gauster *et al.*, Solid State Communications **24**, 619 (1977).
- <sup>32</sup> ESPI Metals, 1050 Benson Way, Ashland, Oregon 97520, USA.
- <sup>33</sup> S.R. Dunsiger *et al.*, Phys. Rev. B **73**, 172418 (2006).
- <sup>34</sup> J. F. Ziegler, Nucl. Instrum. Methods B **219**, 1027 (2004).
- <sup>35</sup> J.F. Bueno *et al.*, Phys. Rev. D (to be submitted); J.F. Bueno, PhD. Thesis, University of British Columbia, 2010 (<http://hdl.handle.net/2429/23724>).